Structure and Equation of State of Neutron-Star Crusts

Nicolas Chamel

Institute of Astronomy and Astrophysics
Université Libre de Bruxelles, Belgium

in collaboration with:
J. M. Pearson, A. F. Fantina, S. Goriely, Y. D. Mutafchieva, Zh. Stoyanov

Compact stars and gravitational waves, Kyoto, 31 October - 4 November 2016

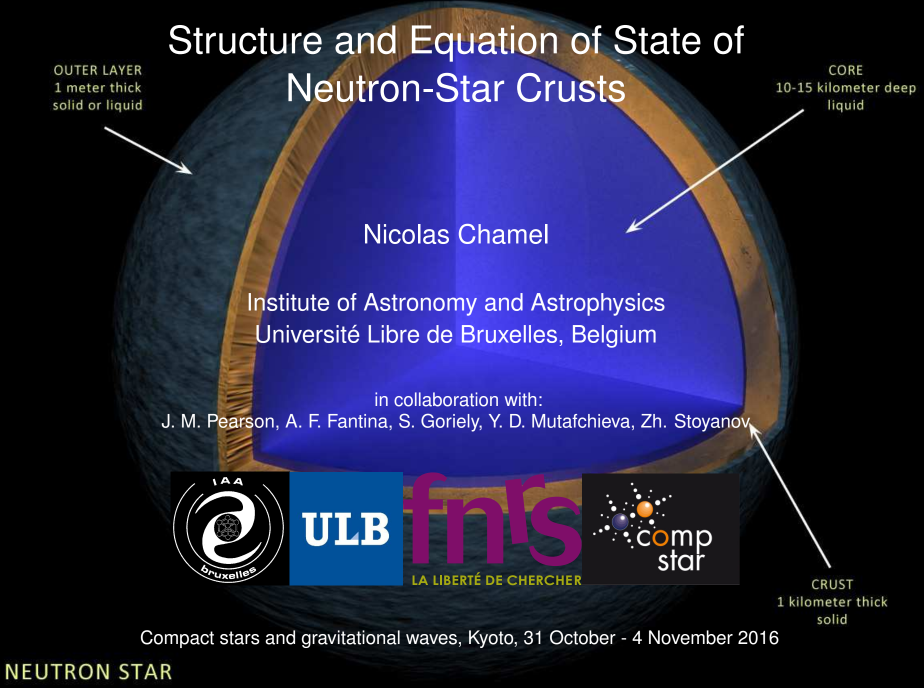

Prelude

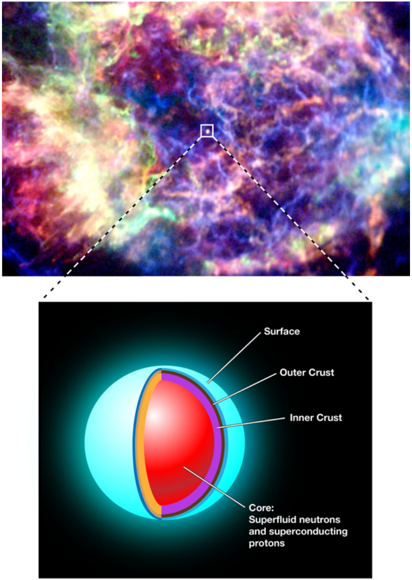

Although the crust of a neutron star represents about $\sim$ 1% of the mass and $\sim$ 10% of the radius, it is related to various phenomena:

- pulsar sudden spin-ups,
- X-ray (super)bursts,
- thermal relaxation in transiently accreting stars,
- quasiperiodic oscillations in soft gamma-ray repeaters
- r-process nucleosynthesis in neutron-star mergers (see Janka's talk)
- mountains and gravitational wave emission

Plumbing neutron-star crusts

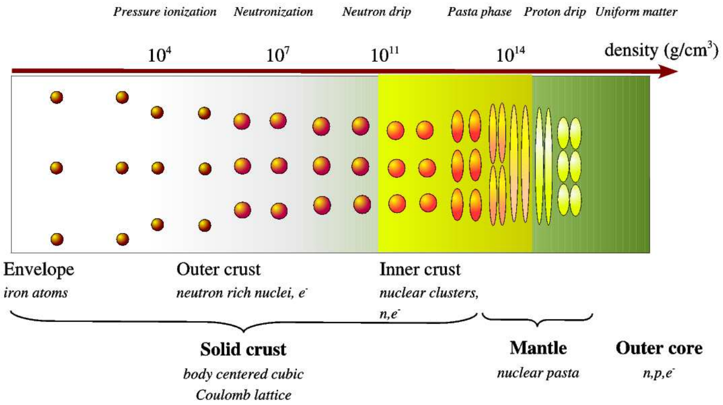

Chamel&Haensel, Living Reviews in Relativity 11 (2008), 10
http://relativity.livingreviews.org/Articles/lrr-2008-10/

The **nuclear energy density functional theory** provides a consistent and numerically tractable treatment of all these different phases.

Outline

1. Nuclear energy density functionals for astrophysics
   - nuclear energy-density functional theory
   - Brussels-Montreal functionals

2. Applications to neutron-star crusts
   - composition and equation of state
   - role of a high magnetic field
   - neutron conduction (entrainment)
   - glitch puzzle

Nuclear energy density functional theory in a nut shell

The energy $E[n_q(\boldsymbol{r}), \widetilde{n_q}(\boldsymbol{r})]$ of a nuclear system ($q = n, p$ for neutrons, protons) can be expressed as a (universal) *functional* of

- "normal" nucleon number densities $n_q(\boldsymbol{r})$,
- "abnormal" densities $\widetilde{n_q}(\boldsymbol{r})$ (roughly the density of paired nucleons of charge q).

In turn these densities are written in terms of **independent quasiparticle wave functions** $\varphi_{1k}^{(q)}(\boldsymbol{r})$ and $\varphi_{2k}^{(q)}(\boldsymbol{r})$ as

$$n_q(\boldsymbol{r}) = \sum_{k(q)} \varphi_{2k}^{(q)}(\boldsymbol{r})\varphi_{2k}^{(q)}(\boldsymbol{r})^*\,, \qquad \widetilde{n_q}(\boldsymbol{r}) = -\sum_{k(q)} \varphi_{2k}^{(q)}(\boldsymbol{r})\varphi_{1k}^{(q)}(\boldsymbol{r})^*$$

The ***exact* ground-state energy** can be obtained by minimizing the energy functional $E[n_q(\boldsymbol{r}), \widetilde{n_q}(\boldsymbol{r})]$ under the constraint of fixed nucleon numbers (and completeness relations on $\varphi_{1k}^{(q)}(\boldsymbol{r})$ and $\varphi_{2k}^{(q)}(\boldsymbol{r})$).

Duguet, Lecture Notes in Physics 879 (Springer-Verlag, 2014), p. 293

Dobaczewski & Nazarewicz, in "50 years of Nuclear BCS" (World Scientific Publishing, 2013), pp.40-60

Skyrme effective nucleon-nucleon interactions

Functionals can be constructed from **generalized** **Skyrme effective interactions**

$$
\begin{aligned}
v_{ij} = {} & t_0(1 + x_0 P_\sigma)\delta(\boldsymbol{r}_{ij}) + \frac{1}{2} t_1(1 + x_1 P_\sigma)\frac{1}{\hbar^2}\left[p_{ij}^2\,\delta(\boldsymbol{r}_{ij}) + \delta(\boldsymbol{r}_{ij})\,p_{ij}^2\right] \\
& + t_2(1 + x_2 P_\sigma)\frac{1}{\hbar^2}\boldsymbol{p}_{ij}.\delta(\boldsymbol{r}_{ij})\,\boldsymbol{p}_{ij} + \frac{1}{6} t_3(1 + x_3 P_\sigma) n(\boldsymbol{r})^\alpha\,\delta(\boldsymbol{r}_{ij}) \\
& + \frac{1}{2} t_4(1 + x_4 P_\sigma)\frac{1}{\hbar^2}\left\{p_{ij}^2\, n(\boldsymbol{r})^\beta\,\delta(\boldsymbol{r}_{ij}) + \delta(\boldsymbol{r}_{ij})\, n(\boldsymbol{r})^\beta\, p_{ij}^2\right\} \\
& + t_5(1 + x_5 P_\sigma)\frac{1}{\hbar^2}\boldsymbol{p}_{ij}\cdot n(\boldsymbol{r})^\gamma\,\delta(\boldsymbol{r}_{ij})\,\boldsymbol{p}_{ij} \\
& + \frac{\mathrm{i}}{\hbar^2} W_0(\boldsymbol{\sigma_i} + \boldsymbol{\sigma_j})\cdot\boldsymbol{p}_{ij}\times\delta(\boldsymbol{r}_{ij})\,\boldsymbol{p}_{ij} + \frac{\mathrm{i}}{\hbar^2} W_1(\boldsymbol{\sigma}_i + \boldsymbol{\sigma}_j)\cdot\boldsymbol{p}_{ij}\times(n_{qi} + n_{qj})^\nu\,\delta(\boldsymbol{r}_{ij})\,\boldsymbol{p}_{ij}
\end{aligned}
$$

$$
\textbf{pairing}\quad v_{ij}^\pi = \frac{1}{2}(1 + P_\sigma)\, v^\pi[n_n(\boldsymbol{r}), n_p(\boldsymbol{r})]\,\delta(\boldsymbol{r}_{ij})
$$

$\boldsymbol{r}_{ij} = \boldsymbol{r}_i - \boldsymbol{r}_j$, $\boldsymbol{r} = (\boldsymbol{r}_i + \boldsymbol{r}_j)/2$, $\boldsymbol{p}_{ij} = -\mathrm{i}\hbar(\boldsymbol{\nabla}_i - \boldsymbol{\nabla}_j)/2$ is the relative momentum, and P_σ is the two-body spin-exchange operator.

The parameters t_i, x_i, α, β, γ, ν, W_i must be fitted to some experimental and/or microscopic nuclear data.

Brussels-Montreal Skyrme functionals (BSk)

These functionals were fitted to both experimental data and N-body calculations using realistic interactions.

Experimental data:

- all atomic masses with $Z, N \geq 8$ from the Atomic Mass Evaluation (root-mean square deviation: 0.5-0.6 MeV)
- nuclear charge radii
- incompressibility $K_v = 240 \pm 10$ MeV (ISGMR)
  Colò et al., Phys.Rev.C70, 024307 (2004).

N-body calculations using realistic forces:

- equation of state of pure neutron matter
- ${}^1S_0$ pairing gaps in nuclear matter
- effective masses in nuclear matter
- stability against spin and spin-isospin fluctuations

Chamel et al., Acta Phys. Pol. B46, 349(2015)

Brussels-Montreal Skyrme functionals

Main features of the latest functionals:

- **fit to realistic $^1S_0$ pairing gaps (no self-energy)** (BSk16-17)
  Chamel, Goriely, Pearson, Nucl.Phys.A812,72 (2008)
  Goriely, Chamel, Pearson, PRL102,152503 (2009).
- **removal of spurious spin-isospin instabilities** (BSk18)
  Chamel, Goriely, Pearson, Phys.Rev.C80,065804(2009)
- **fit to realistic neutron-matter equations of state** (BSk19-21)
  Goriely, Chamel, Pearson, Phys.Rev.C82,035804(2010)
- **fit to different symmetry energies** (BSk22-26)
  Goriely, Chamel, Pearson, Phys.Rev.C88,024308(2013)
- **optimal fit of the 2012 AME** - rms 0.512 MeV (BSk27*)
  Goriely, Chamel, Pearson, Phys.Rev.C88,061302(R)(2013)
- **generalized spin-orbit coupling** (BSk28-29)
  Goriely, Nucl.Phys.A933,68(2015).
- **fit to realistic $^1S_0$ pairing gaps with self-energy** (BSk30-32)
  Goriely, Chamel, Pearson, Phys.Rev. C93,034337(2016).

Neutron-matter equation of state

The neutron-matter equation of state obtained with our functionals are consistent with microscopic calculations using realistic interactions:

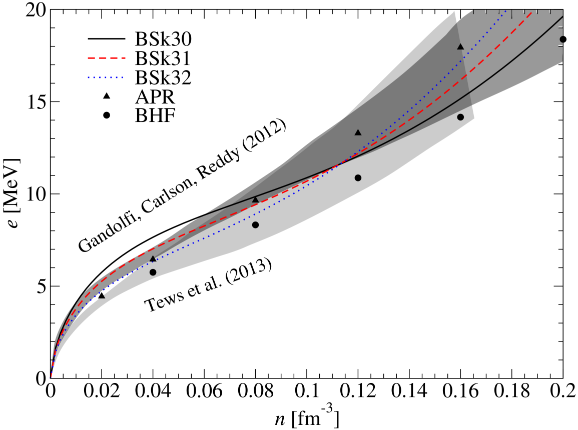

See Gandolfi and Baldo's talks, poster I-4

Symmetry energy

The values for the symmetry energy J and its slope L obtained with our functionals are consistent with various experimental constraints. **The dashed line delimits the values from 30 different HFB atomic mass models with rms** < 0.84 **MeV.**

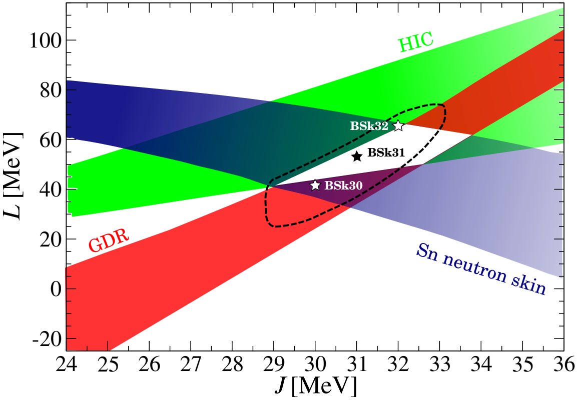

Figure adapted from *Lattimer& Steiner, EPJA50,40(2014)*

Symmetric nuclear-matter equation of state

Our functionals are also in compatible with empirical constraints inferred from heavy-ion collisions:

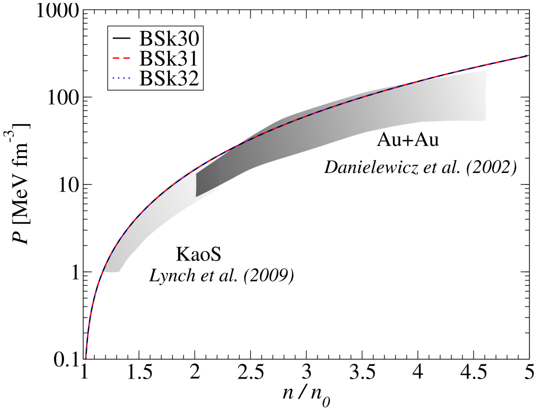

Danielewicz et al., Science 298, 1592 (2002)

Lynch et al., Prog. Part. Nuc. Phys.62, 427 (2009)

Nucleon effective masses

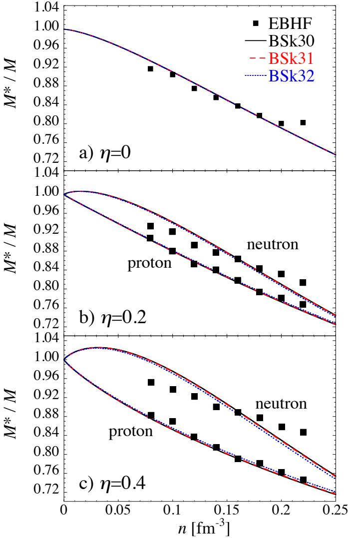

Effective masses obtained with our functionals are consistent with giant resonances in finite nuclei and many-body calculations in infinite nuclear matter.

This was achieved using generalized Skyrme interactions with density dependent t_1 and t_2 terms, initially introduced to remove spurious instabilities.
Chamel, Goriely, Pearson, Phys.Rev.C80,065804(2009)

EBHF calculations from *Cao et al.,Phys.Rev.C73,014313(2006)*.

Description of the outer crust of a neutron star

Main assumptions:

- atoms are fully pressure ionized $\rho \gg 10AZ$ g cm^{-3}
- the crust consists of a perfect body-centered cubic crystal
  $T < T_m \approx 1.3 \times 10^5 Z^2 \left(\frac{\rho_6}{A}\right)^{1/3}$ K $\qquad \rho_6 \equiv \rho/10^6$ g cm^{-3}
- electrons are uniformly distributed and are highly degenerate
- matter is fully "catalyzed"

The only microscopic inputs are nuclear masses. We have made use of the experimental data from the Atomic Mass Evaluation complemented with our HFB mass tables available at
`http://www.astro.ulb.ac.be/bruslib/`

Pearson,Goriely,Chamel,Phys.Rev.C83,065810(2011)

Electron polarization effects are included using the expressions given by *Chamel & Fantina,Phys.Rev.D93, 063001 (2016)*

Composition of the outer crust of a neutron star

The composition of the crust is completely determined by experimental nuclear masses down to about 200m for a $1.4 M_{\odot}$ neutron star with a 10 km radius

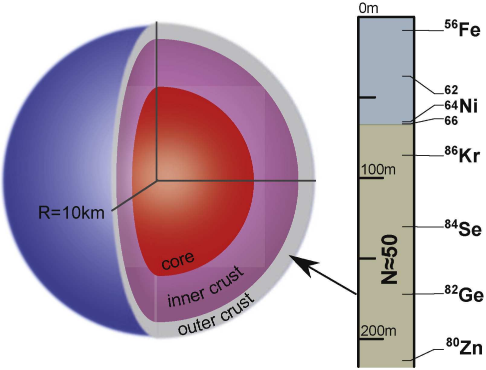

Pearson,Goriely,Chamel,Phys.Rev.C83,065810(2011)
Kreim, Hempel, Lunney, Schaffner-Bielich, Int.J.M.Spec.349-350,63(2013)
Wolf et al.,PRL 110,041101(2013)

Composition of the outer crust of a neutron star

Role of the symmetry energy

HFB-22-25 were fitted to different values of the symmetry energy coefficient at saturation, from $J = 29$ MeV (HFB-25) to $J = 32$ MeV (HFB-22).

HFB-22 (32)	HFB-24 (30)	HFB-25 (29)
^{79}Cu	-	-
^{82}Zn	-	-
^{78}Ni	^{78}Ni	^{78}Ni
^{80}Ni	^{80}Ni	-
-	-	^{126}Ru
^{124}Mo	^{124}Mo	^{124}Mo
^{122}Zr	^{122}Zr	^{122}Zr
^{121}Y	^{121}Y	^{121}Y
-	^{120}Sr	^{120}Sr
^{122}Sr	^{122}Sr	^{122}Sr
^{124}Sr	^{124}Sr	-
^{128}Sr	-	-

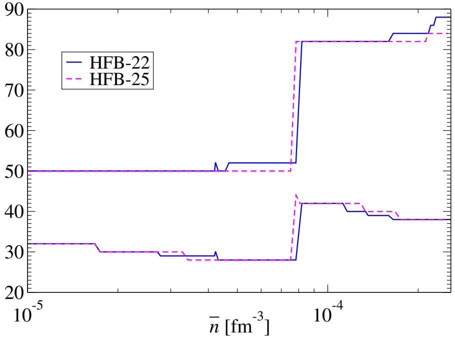

Composition of the outer crust of a neutron star

Role of the symmetry energy

HFB-22-25 were fitted to different values of the symmetry energy coefficient at saturation, from $J = 29$ MeV (HFB-25) to $J = 32$ MeV (HFB-22).

HFB-22 (32)	HFB-24 (30)	HFB-25 (29)
^{79}Cu	-	-
^{82}Zn	-	-
^{78}Ni	^{78}Ni	^{78}Ni
^{80}Ni	^{80}Ni	-
-	-	^{126}Ru
^{124}Mo	^{124}Mo	^{124}Mo
^{122}Zr	^{122}Zr	^{122}Zr
^{121}Y	^{121}Y	^{121}Y
-	^{120}Sr	^{120}Sr
^{122}Sr	^{122}Sr	^{122}Sr
^{124}Sr	^{124}Sr	-
^{128}Sr	-	-

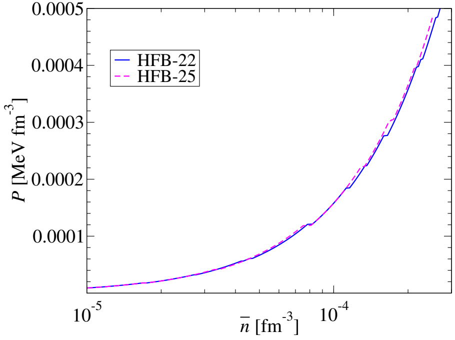

Composition of the outer crust of a neutron star

Role of the spin-orbit coupling

HFB-24: $v^{\rm so}_{ij} = \frac{\rm i}{\hbar^2} W_0(\boldsymbol{\sigma}_i + \boldsymbol{\sigma}_j)\cdot \boldsymbol{p}_{ij} \times \delta(\boldsymbol{r}_{ij})\, \boldsymbol{p}_{ij}$

HFB-28: $v^{\rm so}_{ij} \to v^{\rm so}_{ij} + \frac{\rm i}{\hbar^2} W_1(\boldsymbol{\sigma}_i + \boldsymbol{\sigma}_j)\cdot \boldsymbol{p}_{ij} \times (n_{qi}+n_{qj})^{\nu}\,\delta(\boldsymbol{r}_{ij})\, \boldsymbol{p}_{ij}$

HFB-29: $\mathcal{E}_{\rm so} = \frac{1}{2}\left[\boldsymbol{J}\cdot\nabla n + (1+y_w)\sum_q \boldsymbol{J_q}\cdot\nabla n_q\right]$

HFB-28	HFB-29	HFB-24
^{79}Cu	^{79}Cu	-
^{78}Ni	^{78}Ni	^{78}Ni
^{128}Pd	-	-
^{80}Ni	-	^{80}Ni
^{126}Ru	^{126}Ru	-
^{124}Mo	^{124}Mo	^{124}Mo
^{122}Zr	^{122}Zr	^{122}Zr
-	^{121}Y	^{121}Y
^{120}Sr	^{120}Sr	^{120}Sr
^{122}Sr	^{122}Sr	^{122}Sr
^{124}Sr	^{124}Sr	^{124}Sr

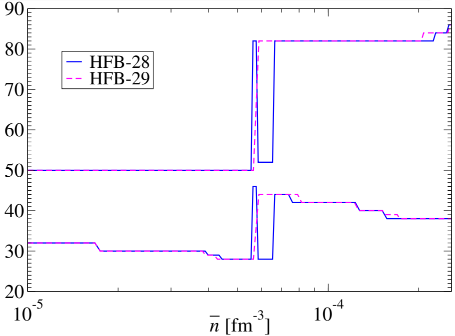

Composition of the outer crust of a neutron star

Role of the spin-orbit coupling

HFB-24: $v_{ij}^{\rm so} = \frac{\rm i}{\hbar^2} W_0(\boldsymbol{\sigma}_i + \boldsymbol{\sigma}_j)\cdot \boldsymbol{p}_{ij} \times \delta(\boldsymbol{r}_{ij})\,\boldsymbol{p}_{ij}$

HFB-28: $v_{ij}^{\rm so} \rightarrow v_{ij}^{\rm so} + \frac{\rm i}{\hbar^2} W_1(\boldsymbol{\sigma}_i + \boldsymbol{\sigma}_j)\cdot \boldsymbol{p}_{ij} \times (n_{qi} + n_{qj})^{\nu}\,\delta(\boldsymbol{r}_{ij})\,\boldsymbol{p}_{ij}$

HFB-29: $\mathcal{E}_{\rm so} = \frac{1}{2}\left[\boldsymbol{J}\cdot\nabla n + (1+y_w)\sum_q \boldsymbol{J_q}\cdot\nabla n_q\right]$

HFB-28	HFB-29	HFB-24
^{79}Cu	^{79}Cu	-
^{78}Ni	^{78}Ni	^{78}Ni
^{128}Pd	-	-
^{80}Ni	-	^{80}Ni
^{126}Ru	^{126}Ru	-
^{124}Mo	^{124}Mo	^{124}Mo
^{122}Zr	^{122}Zr	^{122}Zr
-	^{121}Y	^{121}Y
^{120}Sr	^{120}Sr	^{120}Sr
^{122}Sr	^{122}Sr	^{122}Sr
^{124}Sr	^{124}Sr	^{124}Sr

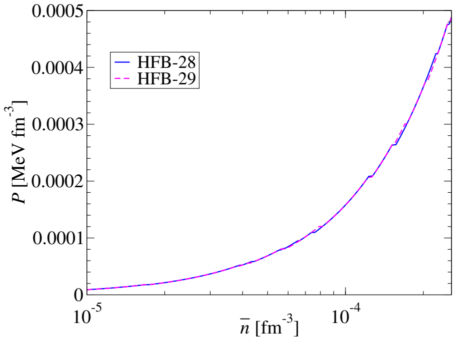

Composition of the outer crust of a neutron star

Role of nuclear pairing

HFB-27* is based on an empirical pairing functional.
HFB-29 (HFB-30) was fitted to EBHF $^1S_0$ pairing gaps including medium polarization effects without (with) self-energy effects.

HFB-27*	HFB-29	HFB-30
-	^{79}Cu	-
^{78}Ni	^{78}Ni	^{78}Ni
-	-	^{80}Ni
^{126}Ru	^{126}Ru	^{126}Ru
^{124}Mo	^{124}Mo	^{124}Mo
^{122}Zr	^{122}Zr	^{122}Zr
-	^{121}Y	^{121}Y
^{120}Sr	^{120}Sr	^{120}Sr
^{122}Sr	^{122}Sr	^{122}Sr
^{124}Sr	^{124}Sr	^{124}Sr

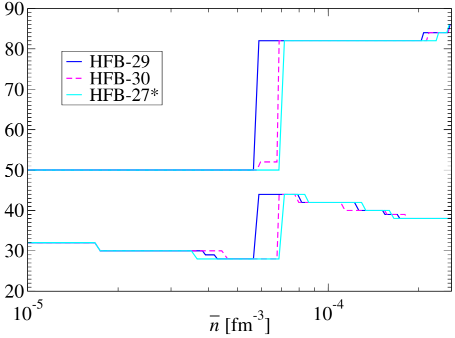

Composition of the outer crust of a neutron star

Role of nuclear pairing

HFB-27* is based on an empirical pairing functional.
HFB-29 (HFB-30) was fitted to EBHF $^1S_0$ pairing gaps including medium polarization effects without (with) self-energy effects.

HFB-27*	HFB-29	HFB-30
-	^{79}Cu	-
^{78}Ni	^{78}Ni	^{78}Ni
-	-	^{80}Ni
^{126}Ru	^{126}Ru	^{126}Ru
^{124}Mo	^{124}Mo	^{124}Mo
^{122}Zr	^{122}Zr	^{122}Zr
-	^{121}Y	^{121}Y
^{120}Sr	^{120}Sr	^{120}Sr
^{122}Sr	^{122}Sr	^{122}Sr
^{124}Sr	^{124}Sr	^{124}Sr

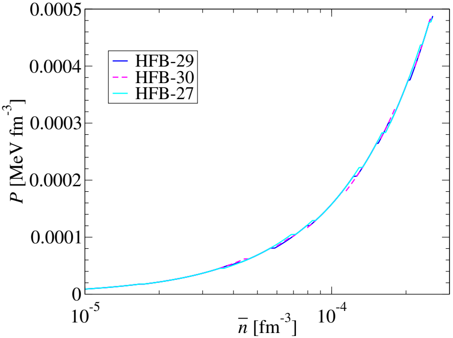

Stratification and equation of state

So far, we have assumed pure layers made of only one kind of nuclei

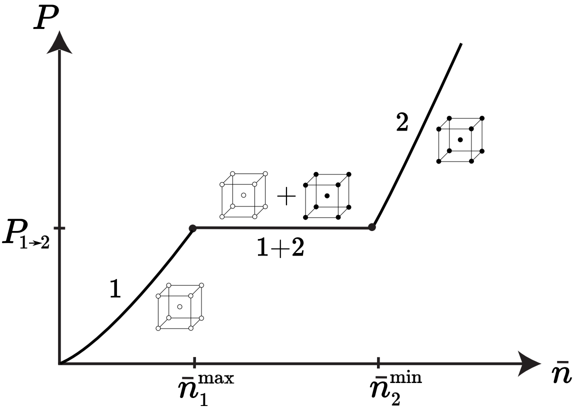

$$\frac{\bar{n}_2^{\min} - \bar{n}_1^{\max}}{\bar{n}_1^{\max}} \approx \frac{A_2}{Z_2}\frac{Z_1}{A_1}\left[1 + \frac{C_{\rm bcc}\alpha}{(3\pi^2)^{1/3}}\left(Z_1^{2/3} - Z_2^{2/3}\right)\right] - 1$$

with $C_{\rm bcc} = -1.444231$ and $\alpha = e^2/\hbar c$

Stratification and equation of state

So far, we have assumed pure layers made of only one kind of nuclei

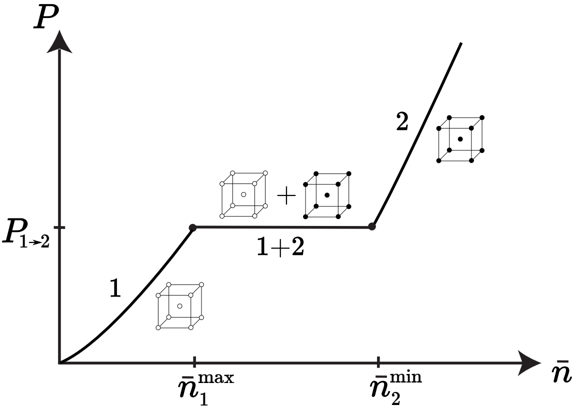

$\dfrac{\bar{n}_2^{\min} - \bar{n}_1^{\max}}{\bar{n}_1^{\max}} > 0 \Rightarrow \dfrac{Z_2}{A_2} < \dfrac{Z_1}{A_1}$: **the denser, the more neutron rich**

Binary compounds in neutron-star crusts?

We have investigated the formation of various ordered binary compounds in the outer crust of a nonaccreting neutron star:

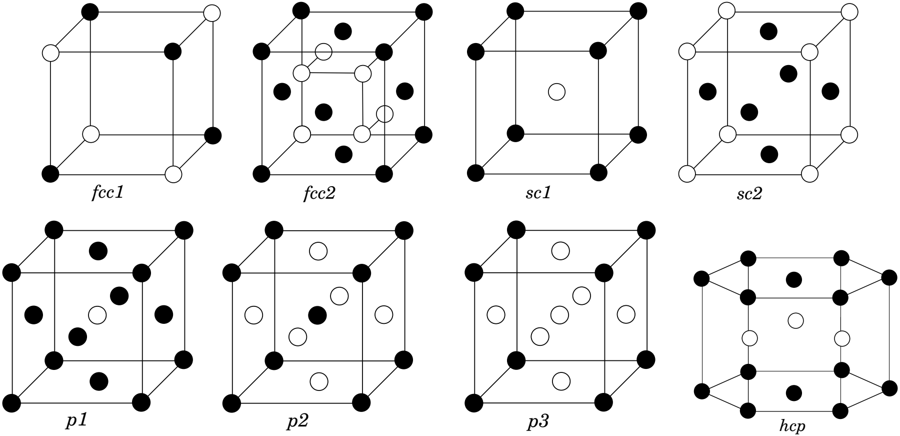

Ternary compounds in neutron-star crusts?

We have also considered ternary compounds with cubic perovskite structure such as $BaTiO_3$:

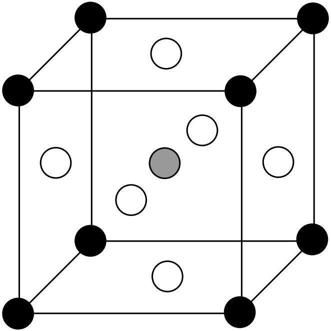

Insterstitial compounds in neutron-star crusts

Compounds with CsCl structure are present at interfaces if $Z_1 \neq Z_2$.

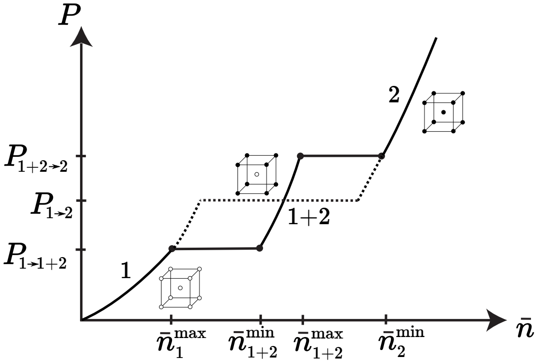

$$\frac{\bar{n}_{1+2}^{\max} - \bar{n}_{1+2}^{\min}}{\bar{n}_2^{\min} - \bar{n}_1^{\max}} \approx \frac{3C_{\rm bcc}\alpha}{(3\pi^2)^{1/3}} \frac{\tilde{f}(Z_1, Z_2) - \dfrac{\overline{Z^{5/3}}}{\bar{Z}}}{\left(1 - \dfrac{\bar{Z}A_1}{\bar{A}Z_1}\right)\left(1 - \dfrac{\bar{Z}A_2}{\bar{A}Z_2}\right)} \ll 1$$

Chamel & Fantina, submitted.

Neutron-drip transition: general considerations

Nuclei are actually stable against neutron emission but are unstable against *electron captures* accompanied by neutron emission

$$^{A}_{Z}\mathrm{X} + \Delta Z e^- \rightarrow ^{A-\Delta N}_{Z-\Delta Z}\mathrm{Y} + \Delta N\, n + \Delta Z\, \nu_e$$

- **nonaccreting neutron stars**
  All kinds of reactions are allowed: the ground state is reached for $\Delta Z = Z$ and $\Delta N = A$

	outer crust	drip line	$\rho_{\rm drip}$ (g cm^{-3})	$P_{\rm drip}$ (dyn cm^{-2})
HFB-19	^{126}Sr (0.73)	^{121}Sr (-0.62)	4.40×10^{11}	7.91×10^{29}
HFB-20	^{126}Sr (0.48)	^{121}Sr (-0.71)	4.39×10^{11}	7.89×10^{29}
HFB-21	^{124}Sr (0.83)	^{121}Sr (-0.33)	4.30×10^{11}	7.84×10^{29}

- **accreting neutron stars**
  Multiple electron captures are very unlikely: $\Delta Z = 1$ ($\Delta N \geq 1$)

	$\rho_{\rm drip}$ (g cm^{-3})	$P_{\rm drip}$ (dyn cm^{-2})
HFB-21	$2.83 - 5.84 \times 10^{11}$	$4.79 - 12.3 \times 10^{29}$

$\rho_{\rm drip}$ and $P_{\rm drip}$ can be expressed by simple analytical formulas.
Chamel, Fantina, Zdunik, Haensel, Phys. Rev. C91,055803(2015).

Impact of a strong magnetic field on the crust?

In a strong magnetic field $\vec{B}$ (along let's say the z-axis), the **electron motion perpendicular to the field is quantized**:

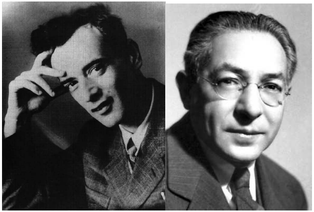

Landau-Rabi levels
Rabi, Z.Phys.49, 507 (1928).

$$e_\nu = \sqrt{c^2 p_z^2 + m_e^2 c^4 (1 + 2\nu B_\star)}$$

where $\nu = 0, 1, ...$ and $\mathbf{B}_\star = \mathbf{B}/\mathbf{B_c}$

with $\mathbf{B_c} = \dfrac{\mathbf{m_e^2 c^3}}{\hbar \mathbf{e}} \simeq \mathbf{4.4} \times \mathbf{10^{13}}$ G.

Maximum number of occupied Landau levels for HFB-21:

$B_\star$	1500	1000	500	100	50	10	1
$\nu_{\rm max}$	1	2	3	14	28	137	1365

Only $\nu = 0$ is filled for $\rho < 2.07 \times 10^6 \left(\dfrac{A}{Z}\right) B_\star^{3/2}$ g cm^{-3}.

Landau quantization can change the properties of the crust.

Equation of state of the outer crust of magnetars

Matter in a magnetar is much more **incompressible and less neutron-rich** than in a neutron star.

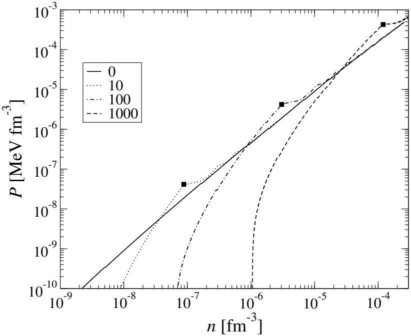

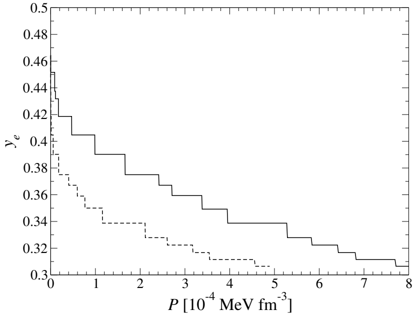

$$P \approx P_0 \left(\frac{n}{n_s} - 1 \right)^2$$

$$y_e \approx \frac{1}{2} \left(1 - \sqrt{\frac{\pi^2 \lambda_e^3 m_e c^2 P}{4 B_\star J^2}} \right)$$

Chamel et al.,Phys.Rev.C86, 055804(2012).

Composition of the outer crust of a magnetar

The magnetic field changes the composition:

Equilibrium nuclides for HFB-24 and $B_\star \equiv B/(4.4 \times 10^{13}\ \mathrm{G})$:

Nuclide	$B_\star$
^{58}Fe(-)	9
^{66}Ni(-)	67
^{88}Sr(+)	859
^{126}Ru(+)	1031
^{80}Ni(-)	1075
^{128}Pd(+)	1445
^{78}Ni(-)	1610
^{79}Cu(-)	1617
^{64}Ni(-)	1668
^{130}Cd(+)	1697
^{132}Sn(+)	1989

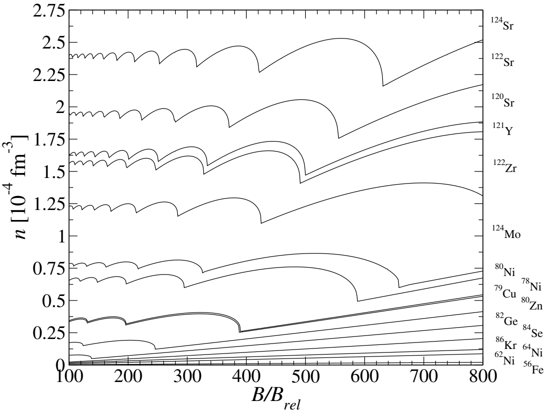

For high enough fields, the crust is almost entirely made of ^{90}Zr.

Neutron-drip transition in magnetars

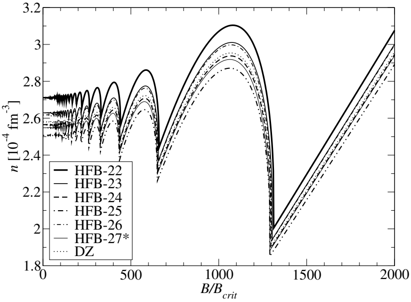

These oscillations are almost universal:

$$\frac{n_{\rm drip}^{\rm min}}{n_{\rm drip}(B_\star=0)} \approx \frac{3}{4}$$

$$\frac{n_{\rm drip}^{\rm max}}{n_{\rm drip}(B_\star=0)} \approx \frac{35+13\sqrt{13}}{72}$$

In the strongly quantizing regime,

$$n_{\rm drip} \approx \frac{A}{Z}\frac{\mu_e^{\rm drip}}{m_e c^2}\frac{B_\star}{2\pi^2\lambda_e^3}\left[1-\frac{4}{3}C\alpha Z^{2/3}\left(\frac{B_\star}{2\pi^2}\right)^{1/3}\left(\frac{m_e c^2}{\mu_e^{\rm drip}}\right)^{2/3}\right]$$

Chamel et al.,Phys.Rev.C91, 065801(2015).
Chamel et al.,J.Phys.:Conf.Ser.724, 012034 (2016).

Neutron-drip transition in magnetars

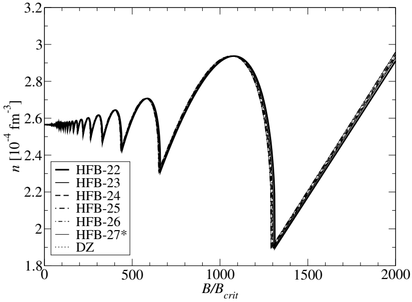

These oscillations are almost universal:

$$\frac{n_{\rm drip}^{\rm min}}{n_{\rm drip}(B_\star=0)} \approx \frac{3}{4}$$

$$\frac{n_{\rm drip}^{\rm max}}{n_{\rm drip}(B_\star=0)} \approx \frac{35+13\sqrt{13}}{72}$$

In the strongly quantizing regime,

$$n_{\rm drip} \approx \frac{A}{Z}\frac{\mu_e^{\rm drip}}{m_e c^2}\frac{B_\star}{2\pi^2\lambda_e^3}\left[1-\frac{4}{3}C\alpha Z^{2/3}\left(\frac{B_\star}{2\pi^2}\right)^{1/3}\left(\frac{m_e c^2}{\mu_e^{\rm drip}}\right)^{2/3}\right]$$

Chamel et al.,Phys.Rev.C91, 065801(2015).
Chamel et al.,J.Phys.:Conf.Ser.724, 012034 (2016).

Neutron-drip transition: role of the symmetry energy

The lack of knowledge of the symmetry energy translates into uncertainties in the neutron-drip density:

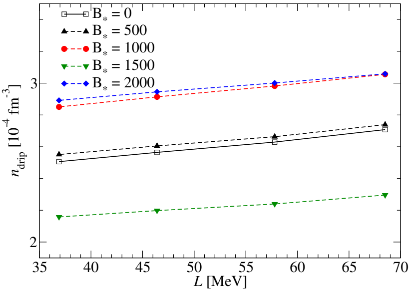

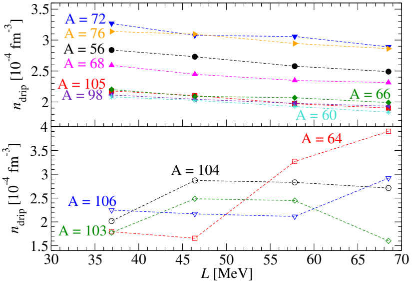

In accreted crusts, the neutron-drip transition may be more sensitive to nuclear-structure effects than the symmetry energy.

Fantina et al.,Phys.Rev.C93,015801(2016).

see poster I-6

Description of neutron star crust beyond neutron drip

We use the **Extended Thomas-Fermi+Strutinsky Integral (ETFSI)** approach with the *same* functional as in the outer crust:

- **semiclassical expansion in powers of $\hbar^2$**: the energy becomes a functional of $n_q(\boldsymbol{r})$ and their gradients only.
- **proton shell effects** are added perturbatively (neutron shell effects are much smaller and therefore neglected).

In order to further speed-up the calculations, clusters are supposed to be spherical (no pastas) and $n_q(\boldsymbol{r})$ are parametrized.

Pearson,Chamel,Pastore,Goriely,Phys.Rev.C91, 018801 (2015).
Pearson,Chamel,Goriely,Ducoin,Phys.Rev.C85,065803(2012).
Onsi,Dutta,Chatri,Goriely,Chamel,Pearson, Phys.Rev.C77,065805 (2008).

Advantages of the ETFSI method:

- very fast approximation to the full HF+BCS equations
- avoids the difficulties related to boundary conditions
  Chamel et al.,Phys.Rev.C75(2007),055806.

Structure of nonaccreting neutron star crusts

With increasing density, the clusters keep essentially the same size but become more and more dilute.

The crust-core transition predicted by the ETFSI method agrees very well with the instability analysis of homogeneous nuclear matter.

	$\bar{n}_{\rm cc}$ (fm^{-3})	$P_{\rm cc}$ (MeV fm^{-3})
BSk27*	0.0919	0.439
BSk25	0.0856	0.211
BSk24	0.0808	0.268
BSk22	0.0716	0.291

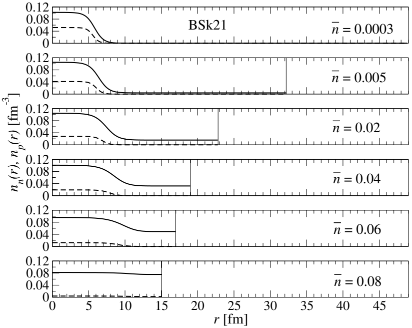

Chamel et al., Acta Phys. Pol.46,349(2015).
Pearson,Chamel,Goriely,Ducoin,Phys.Rev.C85,065803(2012).

The crust-core transition is found to be very smooth.

Role of proton shell effects on the composition of the inner crust of a neutron star

- The ordinary nuclear shell structure seems to be preserved apart from $Z = 40$ (quenched spin-orbit?).
- The energy differences between different configurations become very small as the density increases!

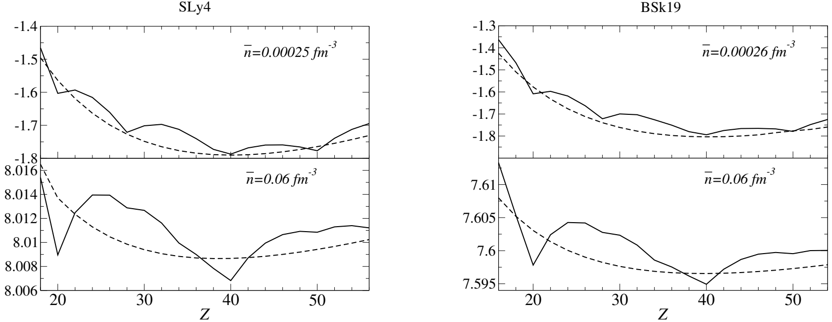

ETF: dashed lines - ETFSI: solid lines

Role of proton pairing on the composition of the inner crust of a neutron star

Proton shell effects are washed out due to pairing.

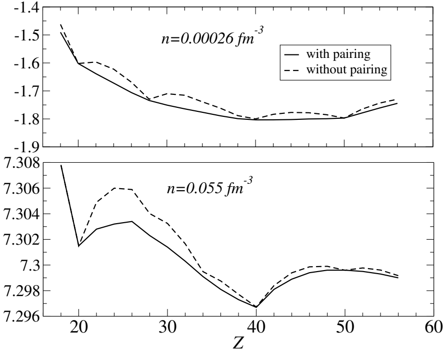

Example with BSk21.

At low densities, $Z = 42$ is energetically favored over $Z = 40$, but by less than 5×10^{-4} MeV per nucleon.

A large range of values of Z could thus be present in a real neutron-star crust.

Pearson,Chamel,Pastore,Goriely,Phys.Rev.C91, 018801 (2015).

Due to proton pairing, the inner crust of a neutron star is expected to contain many impurities.

Unified equations of state of neutron stars

The same functionals used in the crust can be also used in the core (n, p, e^-, μ^-) thus providing a **unified and thermodynamically consistent description of neutron stars**.

- **Tables** of the full equations of state for HFB-19, HFB-20, and HFB-21:

  `http://vizier.cfa.harvard.edu/viz-bin/VizieR?-source=J/A+A/559/A128`

  Fantina, Chamel, Pearson, Goriely, A&A 559, A128 (2013)

- **Analytical representations** of the full equations of state (fortran subroutines):

  `http://www.ioffe.ru/astro/NSG/BSk/`

  Potekhin, Fantina, Chamel, Pearson, Goriely, A&A 560, A48 (2013)

Equations of state for our latest functionals will appear soon.

Bragg scattering and entrainment

For decades, neutron diffraction experiments have been routinely performed to explore the structure of materials.

The main difference in neutron-star crusts is that **neutrons are highly degenerate**

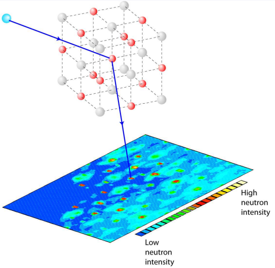

A neutron with wavevector $\boldsymbol{k}$ can be **coherently scattered** if $d \sin\theta = N\pi/k$, where $N = 0, 1, 2, ...$ (Bragg's law).

In this case, it does not propagate in the crystal: it is therefore entrained!

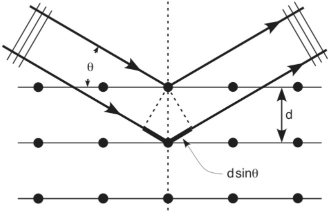

Bragg scattering occurs if $k > \pi/d$. In neutron stars, neutrons have momenta up to k_F. Typically $k_F > \pi/d$ in all regions of the inner crust but the shallowest.

Neutron Fermi surface

Neutron "conduction" depends on the shape of the Fermi surface

Example at $\bar{n} = 0.0003\ \mathrm{fm}^{-3}$ (reduced zone scheme)

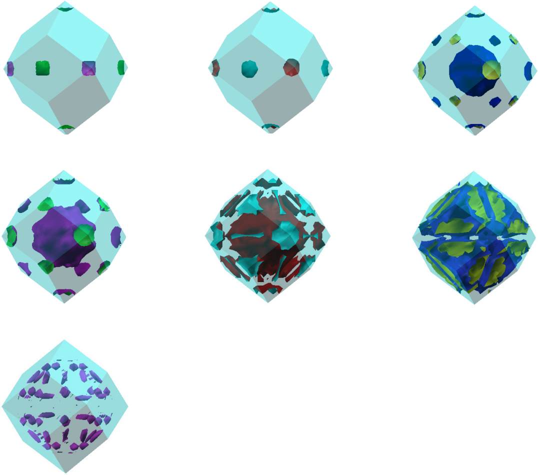

How "free" are neutrons in neutron-star crusts?

Imparting a momentum $\boldsymbol{p_n}$ to "free" neutrons (density n_n^f) induces a neutron current $\boldsymbol{j_n} = n_n^c \boldsymbol{p_n}$ with $n_n^c \neq n_n^f$.

Equivalently $\boldsymbol{p_n} = m_n^\star \boldsymbol{v_n}$ with $m_n^\star = m_n n_n^f / n_n^c$.

$m_n^\star$ (or n_n^c) can be obtained from **band-structure calculations**:

$\bar{n}$ (fm^{-3})	$m_n^\star/m_n$
0.01	6.3
0.02	13.7
0.03	12.7
0.04	9
0.05	2.8
0.06	1.8
0.07	1.2

The density of conduction neutrons is completely determined by the Fermi surface:

$$n_n^c = \frac{m_n}{24\pi^3\hbar^2} \sum_\alpha \int_{\mathrm{F}} |\nabla_{\boldsymbol{k}} \varepsilon_{\alpha \boldsymbol{k}}| \mathrm{d}\mathcal{S}^{(\alpha)} \leq n_n^f$$

Note that n_n^c is a **response function**.

Chamel,Phys.Rev.C85,035801(2012)

How “free” are neutrons in neutron-star crusts?

Imparting a momentum $\boldsymbol{p_n}$ to “free” neutrons (density n_n^f) induces a neutron current $\boldsymbol{j_n} = n_n^c \boldsymbol{p_n}$ with $n_n^c \neq n_n^f$.

Equivalently $\boldsymbol{p_n} = m_n^\star \boldsymbol{v_n}$ with $m_n^\star = m_n n_n^f / n_n^c$.

$m_n^\star$ (or n_n^c) can be obtained from **band-structure calculations**:

$\bar{n}$ (fm^{-3})	$m_n^\star/m_n$
0.01	8.1
0.02	13.7
0.03	12.3
0.04	8.1
0.05	2.2
0.06	1.5
0.07	1.1

role of quantum zero point motion of ions about their equilibrium position?
Kobyakov&Pethick, Phys. Rev. C 87, 055803 (2013)

Including Debye-Waller factor with bare ion mass (overestimate!)
Chamel, in prep.

$m_n^\star$ increased or decreased by $\lesssim 30\%$

How “free” are neutrons in neutron-star crusts?

Imparting a momentum $\boldsymbol{p_n}$ to “free” neutrons (density n_n^f) induces a neutron current $\boldsymbol{j_n} = n_n^c \boldsymbol{p_n}$ with $n_n^c \neq n_n^f$.

Equivalently $\boldsymbol{p_n} = m_n^\star \boldsymbol{v_n}$ with $m_n^\star = m_n n_n^f / n_n^c$.

$m_n^\star$ (or n_n^c) can be obtained from **band-structure calculations**:

$\bar{n}$ (fm^{-3})	$m_n^\star / m_n$
0.01	*on-going*
0.02	15.8
0.03	13.5
0.04	8.2
0.05	2.3
0.06	1.5
0.07	1.1

role of neutron pairing?
Martin&Urban, arXiv:1606.01126 recently found much weaker entrainment using an hydrodynamical approach but only valid if $\xi \ll$ nuclear cluster size.

Including BCS pairing + Debye-Waller factor
preliminary results - weak dependence on the gaps

$m_n^\star$ increased by $\lesssim 15\%$

Entrainment can impact various phenomena (e.g. glitches, QPOs, crust cooling).

Giant pulsar glitches and the inertia of neutron-star superfluids

Giant glitches are usually interpreted as **sudden tranfers of angular momentum between the crustal superfluid and the rest of star**.

Because of entrainment, the superfluid angular momentum reads

$$J_s = I_{ss}\Omega_s + (I_s - I_{ss})\Omega_c$$

(Ω_s and Ω_c being the angular velocities of the superfluid and of the "crust", I_s is the moment of inertia of the superfluid), leading to the following constraint:

$$\frac{I_s}{I} \geq \mathcal{G}\frac{\bar{m}_n^\star}{m_n}\,, \qquad \mathcal{G} = 2\tau_c A_g$$

where $\dfrac{\bar{m}_n^\star}{m_n} = \dfrac{I_{ss}}{I_s}$, $\quad \tau_c = \dfrac{\Omega}{2|\dot{\Omega}|}$ and $A_g = \dfrac{1}{t}\sum_i \dfrac{\Delta\Omega_i}{\Omega}$.

Chamel&Carter,MNRAS368,796(2006)

Vela pulsar glitch constraint

Since 1969, 19 glitches have been regularly detected. The latest one occurred in September 2014.

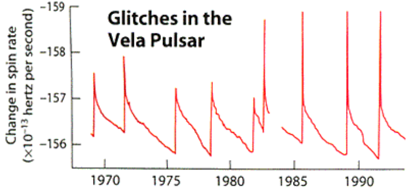

Cumulated glitch amplitude

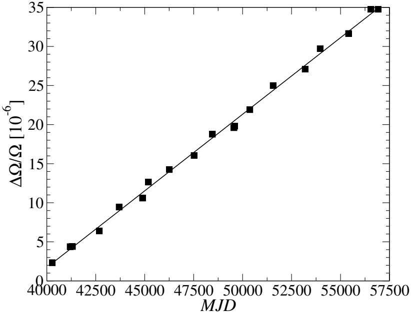

A linear fit of $\dfrac{\Delta\Omega}{\Omega}$ vs t yields

$A_g \simeq 2.25 \times 10^{-14}\ \mathrm{s}^{-1}$

$$\mathcal{G} = 2\tau_c A_g \simeq 1.62\%$$

Glitch puzzle

$\bar{m}_n^\star/m_n = I_{ss}/I_s$ depends mainly on the physics of neutron-star crusts. Using the **thin-crust approximation**, we found $I_{\rm ss} \approx 4.6 I_{\rm crust}$ and $I_{\rm s} \approx 0.89 I_{\rm crust}$ leading to $\bar{m}_n^\star/m_n \approx 5.1$.

The Vela glitch constraint thus becomes $\dfrac{I_s}{I} \geq 8.3\%$, or $\dfrac{I_{\rm crust}}{I} \geq 9.3\%$

The superfluid in the crust of a neutron star with a mass $M > M_\odot$ does not carry enough angular momentum!
Andersson et al., PRL 109, 241103; Chamel, PRL 110, 011101 (2013).

- This conclusion has been confirmed by more recent works, e.g.
  Newton et al, MNRAS 454, 4400 (2015)
  Ang Li et al, ApJS 223, 16 (2016). See poster I-15
- **Could nuclear uncertainties allow for thick enough crusts?**
  Piekarewicz et al.PRC 90, 015803 (2014)
  Steiner et al.PRC 91, 015804 (2015).

Nuclear uncertainties in the mass-radius

Mass-radius relation of nonrotating neutron stars for various *unified* equations of state based on accurately calibrated nuclear models:

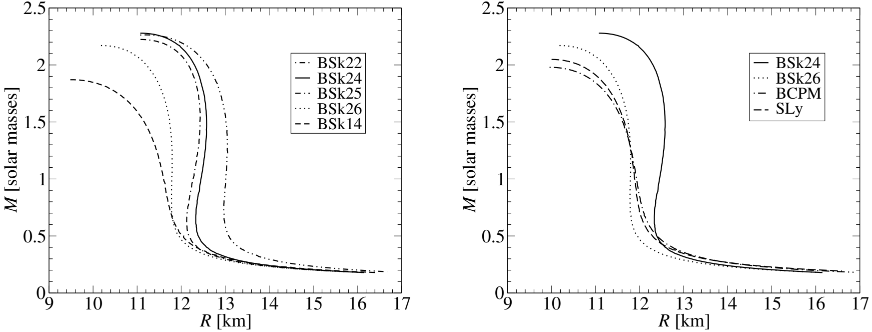

Delsate et al., Phys. Rev. D 94, 023008 (2016)

Refined estimate of the mean effective neutron mass

We have calculated I_s and I_{ss} in the slow-rotation approximation:

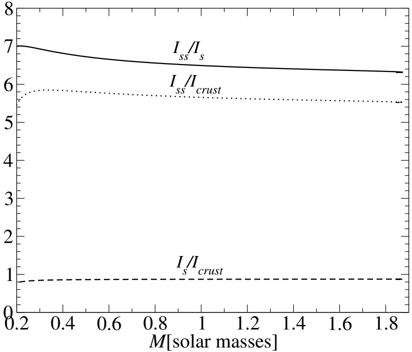

$\bar{m}_n^\star/m_n = I_{ss}/I_s$ is almost independent of the global stellar structure, as expected from the thin-crust approximation. However, the ratio is increased by $\sim 30\%$. We use the same value for all models.

Delsate et al., Phys. Rev. D 94, 023008 (2016)

Nuclear uncertainties and glitch puzzle

We have recalculated $I_{\rm crust}/I$ considering various *unified* equations of state based on accurately calibrated nuclear models:

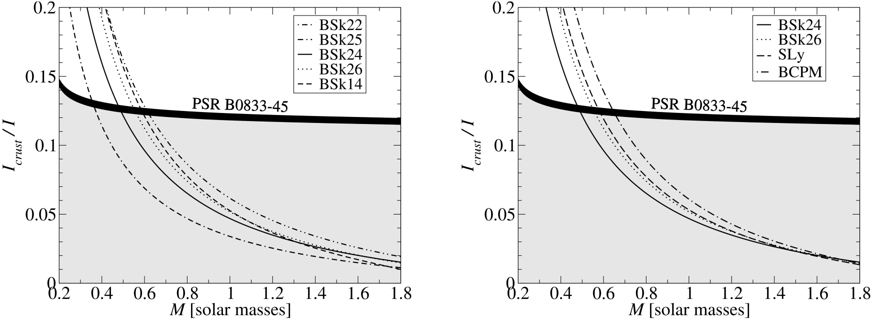

The inferred mass of Vela is at most $0.66 M_\odot$, corresponding to central baryon densities $\bar{n} \approx 0.23 - 0.33$ fm^{-3}. At such densities, the equation of state is fairly well constrained by laboratory experiments.

Delsate et al., Phys. Rev. D 94, 023008 (2016)

Conclusions

- We have developed **accurately calibrated nuclear energy density functionals** fitted to essentially all nuclear mass data as well as to microscopic calculations.
- These functionals provide a **unified and consistent description of neutron-star crusts**.
- **The equation of state of the outer crust is fairly well known**, but its composition depends on the nuclear structure of very exotic nuclei (e.g. spin-orbit coupling, pairing).
- **The constitution of the inner crust is much more uncertain** due to the tiny energy differences between different configurations (nuclear pastas? see Horowitz's talk)
- **Magnetars may have different crusts**.
- **The neutron superfluid is strongly entrained by the crust; this affects various phenomena (glitches, QPOs, cooling)**.

Systematic studies of crustal properties for both nonaccreted and accreted neutron stars are under way.